

Control Variate Score Matching for Diffusion Models

Khaled Kahouli^{1,2,3}, Romuald Elie¹, Klaus-Robert Müller^{1,2,3,4,5}, Quentin Berthet¹,
 Oliver T. Unke ^{*1}, Arnaud Doucet ^{†1}

¹Google DeepMind

²BIFOLD – Berlin Institute for the Foundations of Learning and Data

³Machine Learning Group, Technische Universität Berlin

⁴Department of Artificial Intelligence, Korea University

⁵Max-Planck Institute for Informatics

Abstract

Diffusion models offer a robust framework for sampling from unnormalized probability densities, which requires accurately estimating the score of the noise-perturbed target distribution. While the standard Denoising Score Identity (DSI) relies on data samples, access to the target energy function enables an alternative formulation via the Target Score Identity (TSI). However, these estimators face a fundamental variance trade-off: DSI exhibits high variance in low-noise regimes, whereas TSI suffers from high variance at high noise levels. In this work, we reconcile these approaches by unifying both estimators within the principled framework of *control variates*. We introduce the **Control Variate Score Identity (CVSI)**, deriving an optimal, time-dependent control coefficient that theoretically guarantees variance minimization across the entire noise spectrum. We demonstrate that CVSI serves as a robust, low-variance “plug-in” estimator that significantly enhances sample efficiency in both data-free sampler learning and inference-time diffusion sampling.

1 Introduction & Background

Sampling from unnormalized probability densities $p(\mathbf{x}) \propto e^{-E(\mathbf{x})}$, defined by an energy function $E(\mathbf{x})$, is a fundamental challenge in diverse scientific domains, with applications ranging from molecular dynamics to lattice field theory (Noé et al., 2019; Albergo et al., 2019; Nicoli et al., 2020; Jumper et al., 2021). Diffusion models (Sohl-Dickstein et al., 2015; Ho et al., 2020; Song et al., 2021) have emerged as a robust solution to this problem, reversing a diffusion process that gradually corrupts data with Gaussian noise. Consider a (non-zero and differentiable) distribution $p(\mathbf{x})$ defined on $\mathcal{X} \subseteq \mathbb{R}^d$. The forward process $\{\mathbf{x}(t)\}_{t \in [0,1]}$ is governed by the stochastic differential equation (SDE)

$$d\mathbf{x}(t) = f(t)\mathbf{x}(t) dt + g(t) d\mathbf{w}(t), \quad \mathbf{x}(0) \sim p, \quad (1)$$

where \mathbf{w} denotes the multivariate Wiener process. This SDE defines the marginal probability density path $\{q_t(\mathbf{x})\}_{t \in [0,1]}$ with a closed-form perturbation kernel $q(\mathbf{x}(t)|\mathbf{x}(0)) = \mathcal{N}(\mathbf{x}(t); a(t)\mathbf{x}(0), b(t)^2\mathbf{I})$,

^{*}Corresponding author: oliverunke@google.com

[†]Corresponding author: arnauddoucet@google.com

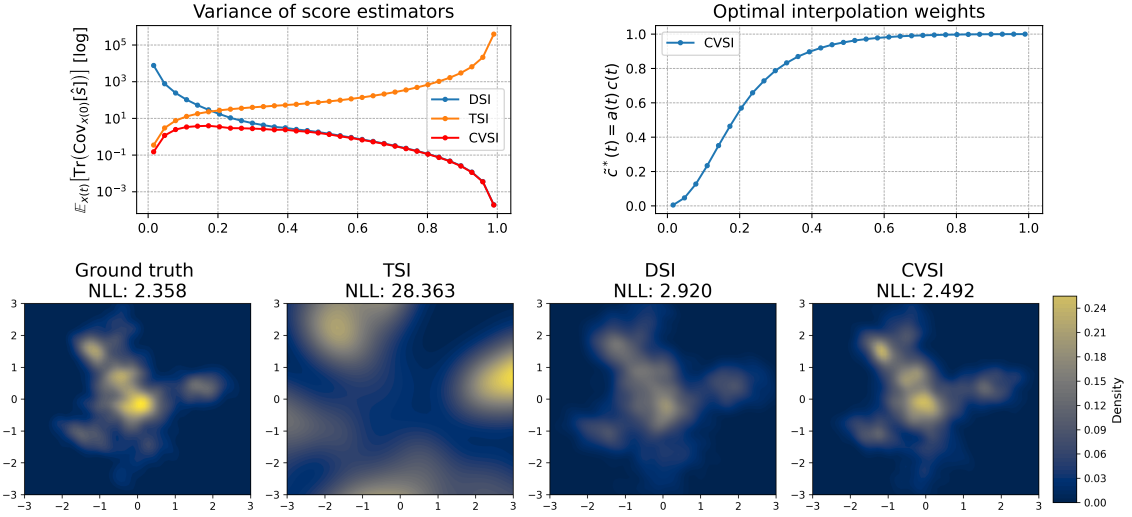


Figure 1: *Top Left:* Variance of the score estimators (log scale) as a function of diffusion time t . DSI (blue) and TSI (orange) exhibit variance explosions at $t \rightarrow 0$ and $t \rightarrow 1$ respectively. Our CVSI (red) consistently achieves the theoretical minimum variance, staying orders of magnitude lower than the baselines in the critical regimes. We use the VP-ISSNR schedule (Kahouli et al., 2025) with $\eta = 1.0$ and $\kappa = 0$. *Top Right:* The derived optimal interpolation weight $\tilde{c}^*(t)$ smoothly transitions from 0 (TSI-dominant) to 1 (DSI-dominant), automatically selecting the stable estimator, dependent on the distribution. *Bottom:* Kernel Density Estimates of samples generated from a 20-component 2D GMM. TSI fails to resolve modes (high NLL), while CVSI recovers the ground truth structure with higher fidelity than DSI (NLL 2.492 vs. Ground Truth 2.358).

where the drift and diffusion coefficients are scalar functions satisfying $f(t) = \dot{a}(t)/a(t)$ and $g^2(t) = 2b(t)/a(t) \left(a(t)\dot{b}(t) - \dot{a}(t)b(t) \right)$, respectively. Sampling is performed by simulating the time-reversed SDE

$$d\tilde{\mathbf{x}}(t) = \left[f(t)\tilde{\mathbf{x}}(t) - \frac{1+\lambda^2}{2}g(t)^2 \nabla_{\tilde{\mathbf{x}}(t)} \log q_t(\tilde{\mathbf{x}}(t)) \right] d\tilde{t} + \lambda g(t) d\tilde{\mathbf{w}}(t), \quad (2)$$

initialized at q_1 where $\tilde{t} = 1 - t$ denotes time reversal. While any $\lambda \geq 0$ yields the same marginal distributions $\{q_t(\mathbf{x})\}_{t \in [0,1]}$, the time-reversal of (1) corresponds to $\lambda = 1$, and the limit $\lambda = 0$ corresponds to the probability flow ODE (Song et al., 2021). Simulating the reverse process requires accurately estimating the score of the noisy marginal distribution, $\nabla_{\mathbf{x}} \log q_t(\mathbf{x})$.

The standard method for estimating this score is the **Denoising Score Identity (DSI)** (Vincent, 2011)

$$\nabla_{\mathbf{x}(t)} \log q_t(\mathbf{x}(t)) = \mathbb{E}_{q(\mathbf{x}(0)|\mathbf{x}(t))} [\nabla_{\mathbf{x}(t)} \log q(\mathbf{x}(t)|\mathbf{x}(0))], \quad (3)$$

where $q(\mathbf{x}(0)|\mathbf{x}(t)) \propto p(\mathbf{x}(0))q(\mathbf{x}(t)|\mathbf{x}(0))$. This identity avoids explicitly evaluating the intractable marginal $q_t(\mathbf{x})$ by conditioning on $\mathbf{x}(0)$. However, DSI is known to suffer from high variance at low noise levels (small t) (De Bortoli et al., 2024). Alternative reparameterizations, such as those derived

from Tweedie’s formula (Robbins, 1992; Efron, 2011) express the score via the clean data expectation

$$\nabla_{\mathbf{x}(t)} \log q_t(\mathbf{x}(t)) = a(t)/b(t)^2 \cdot (\mathbb{E}_{q(\mathbf{x}(0)|\mathbf{x}(t))}[\mathbf{x}(0)] - \mathbf{x}(t)) . \quad (4)$$

However, this formulation does not fundamentally resolve variance amplification near the data manifold ($t \rightarrow 0$). The scaling factor $1/b(t)^2$ diverges in this limit, magnifying estimation errors and resulting in persistent high variance.

In many scientific contexts where \mathbf{x} represents the configuration of a physical system, the unnormalized target score $\nabla_{\mathbf{x}} \log p(\mathbf{x}) = -\nabla_{\mathbf{x}} E(\mathbf{x})$ can be evaluated explicitly, corresponding to the forces acting on the system. Whether used in addition to data samples or as the sole source of information, this quantity allows the marginal score to be expressed via the **Target Score Identity (TSI)**

$$\nabla_{\mathbf{x}(t)} \log q_t(\mathbf{x}(t)) = \frac{1}{a(t)} \mathbb{E}_{q(\mathbf{x}(0)|\mathbf{x}(t))} [\nabla_{\mathbf{x}(0)} \log p(\mathbf{x}(0))] \quad (5)$$

(see (De Bortoli et al., 2024) and Appendix A for the proof). In contrast to DSI, the TSI formulation avoids excessive variance for $t \rightarrow 0$, but instead faces a similar problem at high noise levels (large t), where variance grows rapidly as the correlation between $\mathbf{x}(t)$ and $\mathbf{x}(0)$ vanishes.

To sample from the target p by approximating (2), one must estimate the intractable marginal score $\nabla_{\mathbf{x}(t)} \log q_t(\mathbf{x}(t))$. To do so, Huang et al. (2024); Grenioux et al. (2024) leverage DSI using MCMC samples from $q(\mathbf{x}(0)|\mathbf{x}(t))$, while Akhoun-Sadegh et al. (2024) rely on TSI using an importance sampling approximation of $q(\mathbf{x}(0)|\mathbf{x}(t))$. Alternatively, one can learn a parametric model for the score by minimizing the objective

$$\mathcal{L}(\theta) = \mathbb{E}_{t, \mathbf{x}(t), \mathbf{x}(0)} [w(t) \|\mathbf{s}_\theta(\mathbf{x}(t), t) - \mathbf{s}_{\text{target}}(\mathbf{x}(0), \mathbf{x}(t))\|^2] , \quad (6)$$

where $\mathbf{s}_{\text{target}}(\mathbf{x}(0), \mathbf{x}(t))$ represents the stochastic target derived from the chosen identity. DSI relies on $\mathbf{s}_{\text{target}}(\mathbf{x}(0), \mathbf{x}(t)) = \nabla_{\mathbf{x}(t)} \log q(\mathbf{x}(t)|\mathbf{x}(0))$ (Vincent, 2011) and TSI on $\mathbf{s}_{\text{target}}(\mathbf{x}(0), \mathbf{x}(t)) = \nabla_{\mathbf{x}(0)} \log p(\mathbf{x}(0))$ (De Bortoli et al., 2024). However, by relying either on the TSI or DSI identities, these strategies still suffer from diverging variance at low or high noise levels (small, respectively large t). To mitigate this problem, De Bortoli et al. (2024) and Phillips et al. (2024) proposed a regression target which is a weighted combination of $\nabla_{\mathbf{x}(0)} \log p(\mathbf{x}(0))$ and $\nabla_{\mathbf{x}(t)} \log q(\mathbf{x}(t)|\mathbf{x}(0))$ to reduce variance across noise levels. However, this approach relies on heuristic weighting schedules that lack a theoretical justification for variance minimization. A linear combination of such regression targets is also implicitly exploited by adjoint sampling (Havens et al., 2025).

We rigorously resolve the trade-off between DSI and TSI by unifying both identities within the *control variates* framework (Lemieux, 2014). The resulting **Control Variate Score Identity (CVSI)** features an optimal, time-dependent control coefficient $c^*(t)$ that is theoretically guaranteed to minimize variance (Figure 1). Empirically, CVSI serves as a robust “plug-in” replacement for standard estimators, significantly improving sample efficiency in both data-free training and reverse diffusion sampling. Note that while finalizing this manuscript, we became aware of the concurrent work of Ko and Geffner (2025) which proposes a similar estimator. Our alternative derivation relies on control variates and demonstrate the benefits of this approach for Monte Carlo sampling.

2 Control Variate Score Matching

We resolve the variance trade-off at opposing noise levels by unifying score estimation within the method of *control variates* (Lemieux, 2014) and propose the Control Variate Score Identity (CVSI), a family of

unbiased estimators governed by an optimal, time-dependent control coefficient. This formulation not only theoretically minimizes variance, but also naturally interpolates between DSI and TSI, recovering them as limiting cases of a single, optimal objective.

2.1 Variance Reduction via Control Variates

To reduce the variance of the TSI estimator in Eq. (5), we seek a function $h(\mathbf{x}(0), t)$ that is highly correlated with the primary integrand $g(\mathbf{x}(0), t) = a(t)^{-1} \nabla_{\mathbf{x}(0)} \log p(\mathbf{x}(0))$ and possesses a known expectation under the posterior $q(\mathbf{x}(0)|\mathbf{x}(t))$. We propose using the score of the posterior distribution itself as the control variate:

$$h(\mathbf{x}(0), t) = \nabla_{\mathbf{x}(0)} \log q(\mathbf{x}(0)|\mathbf{x}(t)), \quad (7)$$

because it is linearly related to the target score via Bayes' rule, ensuring high correlation, while standard regularity conditions guarantee that $\mathbb{E}_{q(\mathbf{x}(0)|\mathbf{x}(t))}[h(\mathbf{x}(0), t)] = 0$ (see Appendix A for details). We now formally define our general class of CVSI estimators.

Proposition 1 (Unbiased Control Variate Estimator). *For any time-dependent scalar coefficient $c(t) \in \mathbb{R}$, the following estimator is an unbiased estimator of the marginal score $\nabla_{\mathbf{x}(t)} \log q_t(\mathbf{x}(t))$:*

$$\hat{s}_{\text{CV}}(\mathbf{x}(t)) = \mathbb{E}_{q(\mathbf{x}(0)|\mathbf{x}(t))} \left[\frac{1}{a(t)} \nabla_{\mathbf{x}(0)} \log p(\mathbf{x}(0)) - c(t) \nabla_{\mathbf{x}(0)} \log q(\mathbf{x}(0)|\mathbf{x}(t)) \right]. \quad (8)$$

Proof. See Appendix C. The result follows immediately from the linearity of the expectation and the zero-mean property of the posterior score. \square

This proposition establishes a family of valid score estimators parameterized by $c(t)$. The variance of this estimator is determined by the choice of this coefficient.

2.2 Optimal Control Coefficient

Given the previous control variate formulation, we can derive the optimal time-dependent coefficient $c(t)$ that minimizes the variance of the estimator in Proposition 1. While the score function is vector-valued, we seek a scalar coefficient $c(t)$. In the following propositions, we use the sum of the variances of the individual vector components (equivalently, the trace of the covariance matrix), where for any vector-valued random variables $\mathbf{u}, \mathbf{v} \in \mathbb{R}^d$, we denote the generalized variance and covariance scalars as $\text{Var}(\mathbf{u}) := \mathbb{E}[\|\mathbf{u} - \mathbb{E}[\mathbf{u}]\|^2] = \text{Tr}(\Sigma_{\mathbf{u}})$ and $\text{Cov}(\mathbf{u}, \mathbf{v}) := \mathbb{E}[\langle \mathbf{u} - \mathbb{E}[\mathbf{u}], \mathbf{v} - \mathbb{E}[\mathbf{v}] \rangle] = \text{Tr}(\Sigma_{\mathbf{uv}})$.

Proposition 2 (Optimal Control Coefficient). *The variance of the estimator $\hat{s}_{\text{CV}}(\mathbf{x}(t))$ in Proposition 1 is minimized by the optimal time-dependent coefficient $c^*(t)$:*

$$c^*(t) = \frac{\text{Cov}(a(t)^{-1} \nabla_{\mathbf{x}(0)} \log p(\mathbf{x}(0)), \nabla_{\mathbf{x}(0)} \log q(\mathbf{x}(0)|\mathbf{x}(t)))}{\text{Var}(\nabla_{\mathbf{x}(0)} \log q(\mathbf{x}(0)|\mathbf{x}(t)))}, \quad (9)$$

where the covariance and variance are computed w.r.t. $q(\mathbf{x}(0)|\mathbf{x}(t))$.

Proof. See Appendix C.2 for the general derivation of the variance minimum. \square

The expression in Proposition 2 relies on the score of the posterior, which typically does not have a closed form or requires differentiating through the solver. We reformulate this coefficient using the score of the perturbation kernel, which is analytically tractable.

Proposition 3 (Tractable Optimal Coefficient). *The optimal coefficient $c^*(t)$ can be reformulated in terms of the analytical perturbation kernel score $\mathbf{s}_{t|0} = \nabla_{\mathbf{x}(t)} \log q(\mathbf{x}(t)|\mathbf{x}(0))$ and the target score $\mathbf{s}_p = \nabla_{\mathbf{x}(0)} \log p(\mathbf{x}(0))$:*

$$c^*(t) = \frac{\text{Var}(\mathbf{s}_p) - a(t)\text{Cov}(\mathbf{s}_p, \mathbf{s}_{t|0})}{a(t)\text{Var}(\mathbf{s}_p) + a(t)^3\text{Var}(\mathbf{s}_{t|0}) - 2a(t)^2\text{Cov}(\mathbf{s}_p, \mathbf{s}_{t|0})}, \quad (10)$$

where all statistics are taken w.r.t. the posterior $q(\mathbf{x}(0)|\mathbf{x}(t))$.

Proof. See Appendix C.3. \square

Rather than relying on heuristic weighting schemes, $c^*(t)$ provides a rigorous way to dynamically adjust the contribution of the control variate based on the instantaneous correlation between the target score and the posterior score.

Corollary 1 (Boltzmann Target Distribution). *In the case of a Boltzmann distribution defined by an energy function $E(\mathbf{x})$ and temperature parameter τ , such that $p(\mathbf{x}) \propto \exp(-E(\mathbf{x})/\tau)$, the target score is given by $\nabla_{\mathbf{x}} \log p(\mathbf{x}) = -\nabla_{\mathbf{x}} E(\mathbf{x})/\tau$. Substituting the analytical score of the perturbation kernel $\nabla_{\mathbf{x}(t)} \log q(\mathbf{x}(t)|\mathbf{x}(0)) = \frac{a(t)\mathbf{x}(0) - \mathbf{x}(t)}{b(t)^2}$, the optimal coefficient becomes:*

$$c^*(t) = \frac{\frac{1}{\tau^2} \text{Var}(\nabla E) + \frac{a(t)^2}{\tau b(t)^2} \text{Cov}(\nabla E, \mathbf{x}(0))}{\frac{a(t)}{\tau^2} \text{Var}(\nabla E) + \frac{a(t)^5}{b(t)^4} \text{Var}(\mathbf{x}(0)) + \frac{2a(t)^3}{\tau b(t)^2} \text{Cov}(\nabla E, \mathbf{x}(0))}, \quad (11)$$

where ∇E denotes $\nabla_{\mathbf{x}(0)} E(\mathbf{x}(0))$ and all statistics are taken w.r.t. $q(\mathbf{x}(0)|\mathbf{x}(t))$.

This explicit form allows for the direct computation of optimal variance reduction in physical systems where the energy function is known.

2.3 The Interpolated Estimator

The formulation in Proposition 1 unifies previously distinct estimation methods. By using Bayes rule and utilizing the Gaussian symmetry property $\nabla_{\mathbf{x}(0)} \log q(\mathbf{x}(t)|\mathbf{x}(0)) = -a(t)\nabla_{\mathbf{x}(t)} \log q(\mathbf{x}(t)|\mathbf{x}(0))$ in Eq. (8), we arrive at an optimal interpolated estimator.

Corollary 2 (Optimal Score Interpolation). *Let $\tilde{c}(t) = c(t)a(t)$. The estimator can be rewritten as a convex combination:*

$$\begin{aligned} \nabla_{\mathbf{x}(t)} \log q_t(\mathbf{x}(t)) &= \frac{1 - \tilde{c}(t)}{a(t)} \mathbb{E}_{q(\mathbf{x}(0)|\mathbf{x}(t))} [\nabla_{\mathbf{x}(0)} \log p(\mathbf{x}(0))] \\ &\quad + \tilde{c}(t) \mathbb{E}_{q(\mathbf{x}(0)|\mathbf{x}(t))} [\nabla_{\mathbf{x}(t)} \log q(\mathbf{x}(t)|\mathbf{x}(0))]. \end{aligned} \quad (12)$$

Proof. See Appendix B. \square

This corollary reveals that the standard DSI and TSI estimators, as well as previous mixing approaches (De Bortoli et al., 2024), are special cases of our framework (see Table 1), corresponding to suboptimal choices for $\tilde{c}(t)$, since $c^*(t)$ is derived to strictly minimize the variance. We further highlight a critical distinction regarding the TSM Mode Mixing weighting proposed by De Bortoli et al. (2024).

Table 1: Comparison of different score estimators as special cases of the Control Variate Score Identity (CVSI) based on the choice of the weighting function $\tilde{c}(t)$. For the Target Score Matching (TSM) weightings (De Bortoli et al., 2024), σ_{data}^2 denotes the total data variance. Note that σ_{mode}^2 denotes the average intra-mode variance, which requires access to the ground truth mixture parameters.

Estimator	Weighting $\tilde{c}(t)$	Variance Behavior
Target Score Identity (TSI)	0	Grows as $t \rightarrow 1$
Denoising Score Identity (DSI)	1	Grows as $t \rightarrow 0$
TSM Global Mixing (De Bortoli et al., 2024)	$\frac{b(t)^2}{b(t)^2 + a(t)^2 \sigma_{\text{data}}^2}$	Optimal for Single Gaussian
TSM Mode Mixing (De Bortoli et al., 2024)	$\frac{b(t)^2}{b(t)^2 + a(t)^2 \sigma_{\text{mode}}^2}$	Heuristic for GMM (Requires GT)
CVSI (Ours)	$c^*(t)a(t)$	Minimal Variance

It relies on the intra-mode variance σ_{mode}^2 , a quantity that requires explicit knowledge of the ground truth mixture components. Since this information is generally unavailable in practice, it serves as a theoretical baseline. In contrast, our CVSI coefficient $c^*(t)$ is based on tractable statistics, which does not require access to the ground truth.

Notably, the interpolation form with our optimal weight $\tilde{c}^*(t) = c^*(t)a(t)$ mathematically coincides with the mixture weights identified by Ko and Geffner (2025). However, while Ko and Geffner (2025) approach the problem by directly optimizing a linear interpolation between two estimators, our result emerges directly from the control variate framework, where the posterior score acts as the control variate.

3 Applications in Data-Free Learning and Diffusion Sampling

Our CVSI framework serves as a modular plug-in estimator that minimizes the variance to improve the estimation of the marginal score and reduce the sample complexity required.

3.1 Data-Free Training Methods

When learning from an unnormalized density $p(\mathbf{x}) \propto e^{-E(\mathbf{x})}$ without data samples, we must rely on the Target Score Identity (TSI), as in iDEM (Akhound-Sadegh et al., 2024).

Iterated Denoising Energy Matching (iDEM) iDEM (Akhound-Sadegh et al., 2024) trains a diffusion model by minimizing a score matching loss where the target is estimated via Importance Sampling (IS). Given a proposal distribution $\pi(\mathbf{x}(0)|\mathbf{x}(t))$, typically $\mathcal{N}(\mathbf{x}(0); \mathbf{x}(t)/a(t), (b(t)/a(t))^2 \mathbf{I})$, the iDEM estimator, reformulated with respect to the unscaled $\mathbf{x}(t)$, is defined as:

$$\nabla_{\mathbf{x}(t)} \log q_t(\mathbf{x}(t)) = \frac{1}{a(t)} \nabla_{\tilde{\mathbf{x}}(t)} \log \mathbb{E}_{\pi(\mathbf{x}(0)|\tilde{\mathbf{x}}_t)} [p(\mathbf{x}(0))], \quad (13)$$

where $\tilde{\mathbf{x}}(t) = \mathbf{x}(t)/a(t)$ is the scaled variable. As we show in Appendix D.1, this expression is equivalent to an importance sampling estimator of the TSI:

$$\nabla_{\mathbf{x}(t)} \log q_t(\mathbf{x}(t)) \approx \frac{1}{a(t)} \frac{1}{K} \sum_{k=1}^K w(\mathbf{x}^{(k)}(0); \mathbf{x}(t)) \nabla_{\mathbf{x}(0)} \log p(\mathbf{x}^{(k)}(0)), \quad (14)$$

where $\mathbf{x}^{(k)}(0) \sim \pi(\mathbf{x}(0)|\mathbf{x}(t))$ and the importance weights are defined as:

$$w(\mathbf{x}(0); \mathbf{x}(t)) = \frac{q(\mathbf{x}(0)|\mathbf{x}(t))}{\pi(\mathbf{x}(0)|\mathbf{x}(t))} = \frac{p(\mathbf{x}(0))}{a(t)^D q_t(\mathbf{x}(t))}. \quad (15)$$

Since this formulation relies directly on the TSI integrand $\nabla_{\mathbf{x}(0)} \log p(\mathbf{x}(0))$, it inherits its high variance at large noise levels, which is further exacerbated by the variance of the importance weights, increasing the sample complexity.

By observing that iDEM is simply an IS estimator of the expectation in Eq 5, we can plug in our CVSI estimator (Proposition 1) directly to reduce the variance of the quantity being averaged by the importance weights. Specifically, we replace the target score with our interpolated estimator (Corollary 2). However, we use the empirical estimates derived from the importance samples $\mathbf{x}^{(k)}(0) \sim \pi(\mathbf{x}(0)|\mathbf{x}(t))$ to compute the posterior moments used for the coefficient $c^*(t)$. The resulting estimator is given by:

$$\hat{\mathbf{s}}_{\text{CV-iDEM}} = \frac{1}{K} \sum_{k=1}^K w_k \left[\frac{1 - \hat{c}(t)}{a(t)} \nabla \log p(\mathbf{x}^{(k)}(0)) + \hat{c}(t) \nabla \log q(\mathbf{x}(t)|\mathbf{x}^{(k)}(0)) \right], \quad (16)$$

where $\hat{c}(t) = \hat{c}^*(t)a(t)$ is the IS estimated interpolation weight. This substitution stabilizes the training gradient updates by minimizing the variance of the integrand itself. In particular, we compute $\hat{c}^*(t)$ using the unweighted sample variance and covariance of the proposal samples $\mathbf{x}^{(k)}(0)$. While reweighting these statistics by w_k would theoretically target the true posterior variance, we found that using the unweighted statistics yields more stable training dynamics and better results overall. We note that, as with standard iDEM, the use of Self-Normalized Importance Sampling (SNIS) introduces a bias of order $\mathcal{O}(1/K)$ to the score estimate. Furthermore, estimating the control coefficient $\hat{c}^*(t)$ on the same set of samples used to compute the score introduces an additional bias. Despite these finite-sample effects, the variance reduction provided by the control variate significantly improves the learning signal and performance, as illustrated in Section 4.2.

We implement the importance weights using softmax normalization for numerical stability:

$$w_k = \frac{p(\mathbf{x}^{(k)}(0))}{\sum_{j=1}^K p(\mathbf{x}^{(j)}(0))}, \quad (17)$$

which is equivalent to the theoretical importance weights $w(\mathbf{x}^{(k)}(0); \mathbf{x}(t)) \propto p(\mathbf{x}^{(k)}(0))/q_t(\mathbf{x}(t))$ since the normalization constant $q_t(\mathbf{x}(t))$ and the factor $a(t)^D$ cancel in the softmax operation.

3.2 Variance Reduction for Diffusion Sampling

The CVSI framework is equally applicable during inference. In the reverse-time SDE (Eq. 2), the drift term requires the score $\nabla_{\mathbf{x}} \log q_t(\mathbf{x})$. While some techniques rely on a pre-trained neural network $s_{\theta}(\mathbf{x}, t)$, trained via minimization of a reverse Kullback–Leibler divergence (Zhang and Chen, 2022; Berner et al., 2024; Vargas et al., 2023), others rely on Monte Carlo approximation of this score based on DSI (Huang et al., 2024; Grenioux et al., 2024). By replacing the standard score estimate with CVSI, we minimize the variance of the drift term. This results in more accurate trajectories and higher quality samples, as shown in section 4.1, especially in challenging regimes where standard estimators suffer from high noise artifacts.

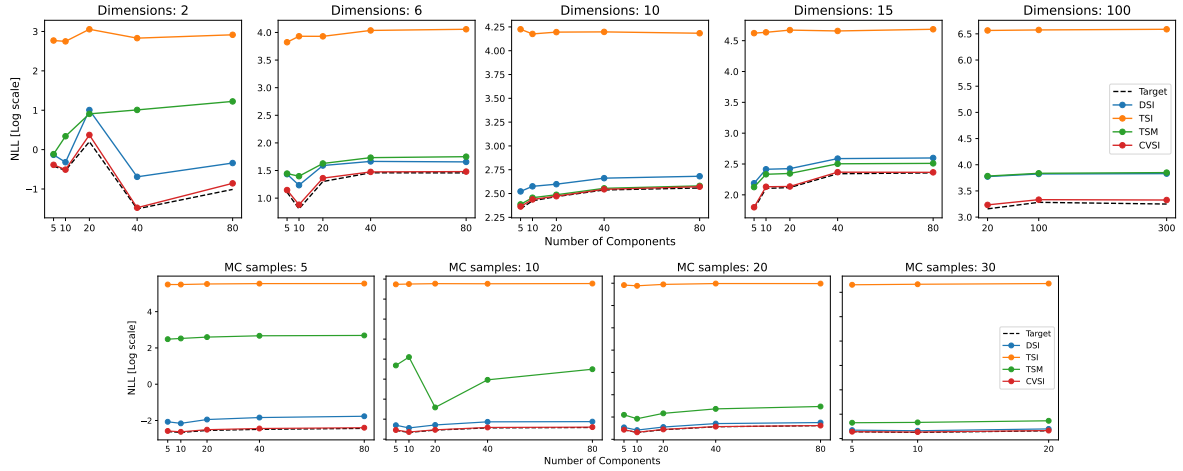


Figure 2: We evaluate the Negative Log-Likelihood (NLL) of samples generated from GMMs of varying complexity, using CVS, TSI, DSI and TSM estimators. *Top Row*: NLL as a function of the number of components for increasing dimensionality $d \in \{2, \dots, 100\}$ (fixed at 10 MC samples). *Bottom Row*: NLL versus component count for varying Monte Carlo (MC) samples per step (fixed at $d = 15$).

4 Experiments

4.1 Sampling

To test the different score estimators in a controlled setting, we use an analytical toy model where the data distribution $p(\mathbf{x})$ is given by a multivariate Gaussian Mixture Model (GMM) in \mathbb{R}^d :

$$p(\mathbf{x}) = \sum_{i=1}^N \pi^i \mathcal{N}(\mathbf{x}; \boldsymbol{\mu}^i, \boldsymbol{\Sigma}^i). \quad (18)$$

To ensure the difficulty of the problem scales appropriately with dimensionality, we generate the mixture parameters randomly, where the mixture weights π^i are drawn uniformly and normalized and the means are sampled from $\boldsymbol{\mu}^i \sim \mathcal{N}(\mathbf{0}, s^2 d \cdot \mathbf{I})$ with scale $s = 10$, ensuring that the modes remain distinguishable as dimension d increases. The covariance matrices are sampled from a Wishart distribution $\boldsymbol{\Sigma}^i \sim \mathcal{W}(\nu, \mathbf{I})$ with degrees of freedom $\nu = 2d$. This setup allows us to control the complexity of the target distribution with the key advantage that the diffused marginal distribution, $q_t(\mathbf{x})$, also remains a GMM for all $t \in [0, 1]$. Consequently, the posterior distribution $q(\mathbf{x}(0) | \mathbf{x}(t))$, which is essential for computing the expectations in the score estimators, admits a closed-form analytical solution. This provides an exact ground truth, enabling a rigorous evaluation where the variance of the estimators can be assessed in the absence of the posterior approximation errors. We provide the full derivations and the explicit formulas for both the marginal and posterior distributions in Appendix E.

Figure 2 summarises the quantitative results of sampling from the target GMMs, where we use the reverse SDE from the TV/SNR framework Kahouli et al. (2025), with $\eta = 1.0$, $\kappa = 0$, $\tau = 1.0$ and $\lambda = 1.0$. We compare the performance of our proposed CVS estimator against the standard baselines, DSI and TSI, and the tractable TSM Global Mixing (De Bortoli et al., 2024). We observe that while

standard estimators like DSI and TSM degrade as the dimension increases to $d = 100$, CVSI maintains a performance profile nearly indistinguishable from the ground truth (Target), suggesting a better scalability with respect to dimensionality. Moreover, CVSI achieves near-optimal NLL with as few as 5 MC samples per step. In contrast, the baselines require significantly larger MC sample sizes (20-30) to achieve comparable stability. This efficiency stems from the optimal control coefficient $c^*(t)$, which minimizes the variance of the estimator itself. This is crucial in many scientific applications, where evaluating the score or energy function is expensive. Figure 1 supports this quantitative assessment, showing that standard estimators often struggle to capture all modes faithfully, whereas CVSI recovers the complex multi-modal structure accurately.

4.2 Training

In this section, we evaluate the effectiveness of our CVSI framework in data-free training scenarios, particularly focusing on the iDEM method (Akhound-Sadegh et al., 2024). We assess how integrating CVSI into iDEM, by using the same IS scheme but replacing the TSI estimator with our CVSI estimator, influences the quality of the learned diffusion models across various energy landscapes.

Implementation Details & Computational Cost For all experiments, we adopt the exact model architectures and training hyperparameters used in Akhound-Sadegh et al. (2024) to ensure a fair comparison. Crucially, our proposed CVSI estimator incurs **no additional computational overhead** compared to the baseline TSI estimator used in iDEM. Both methods require exactly one energy function evaluation per Monte Carlo sample.

Gaussian mixture models We first consider the same Gaussian Mixture Model (GMM) setup used by Akhound-Sadegh et al. (2024), with 40 components in 2D. However, unlike previous experiments that focused on sampling with known posteriors, we focus on training a diffusion sampler directly from the unnormalized density $p(\mathbf{x})$.

Figure 3 presents the results. The quantitative metrics (Left and Center-Left panels) demonstrate that replacing the standard TSI estimator with our CVSI estimator significantly improves sample efficiency. CVSI achieves lower Wasserstein-2 (\mathcal{W}_2) distance and Negative Log-Likelihood (NLL) using far fewer energy function evaluations (NFE) per training sample compared to the baseline. For instance, at low NFE regimes (e.g., 8-32 evaluations), CVSI maintains robust performance while TSI degrades. This quantitative gap translates into a tangible difference in sample quality. The distribution plots (Right panels) show the state of the model trained with limited energy evaluations (NFE=8). The baseline iDEM with TSI suffers from mode dropping. In contrast, iDEM with CVSI successfully covers all 40 modes.

Double-Well potential Similar to Akhound-Sadegh et al. (2024), we evaluate our estimator on the 4-particle Double-Well (DW-4) system. This system consists of $N = 4$ particles in a 2-dimensional space. The energy function is defined by the pairwise distances $d_{ij} = \|\mathbf{x}_i - \mathbf{x}_j\|_2$:

$$\mathcal{E}^{DW}(\mathbf{x}) = \frac{1}{2\tau} \sum_{i,j} (b(d_{ij} - d_0)^2 + c(d_{ij} - d_0)^4). \quad (19)$$

Following Akhound-Sadegh et al. (2024), we use the parameters $b = -4$, $c = 0.9$, $d_0 = 4$, and temperature $\tau = 1$. This potential defines a multi-modal distribution invariant to rotations and permutations, presenting a challenging test for mode coverage.

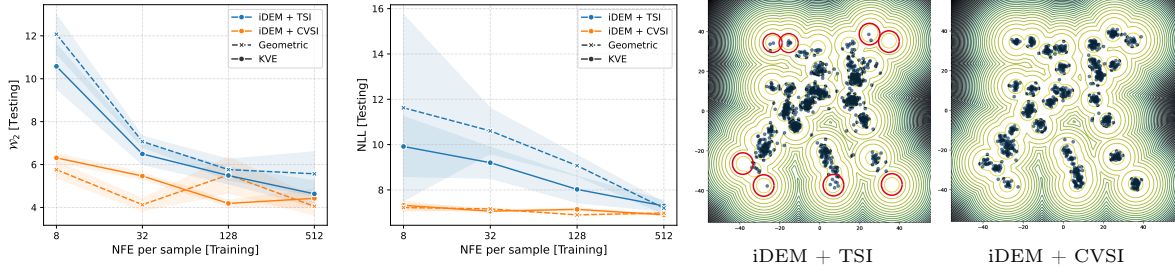


Figure 3: Performance comparison of iDEM with TSI (original) and with our CVSI on the 2D GMM task, using two different schedules, the original geometric schedule (Akhound-Sadegh et al., 2024) and the well-established KVE schedule by (Karras et al., 2022). Metrics include the Wasserstein-2 distance (\mathcal{W}_2) between generated samples and ground truth samples, and the Negative Log-Likelihood (NLL) as a function of the number of energy function evaluations (NFE) used per training sample. The two rightmost plots show the distributions of samples generated by iDEM with TSI (left) and iDEM with CVSI (right) after training with only 8 NFE per training sample. The ground truth distribution is shown as contour lines for reference, problematic modes (deviating strongly from the ground truth) are highlighted with red circles.

Figure 4 summarizes the results. The leftmost plot shows that integrating CVSI into iDEM leads to a faster and more stable minimization of the Wasserstein-2 distance (\mathcal{W}_2) between the generated and ground-truth interatomic distance distributions. The histograms (Center and Right panels) visually confirm this improvement. With fewer NFE, the baseline iDEM+TSI model produces a distribution that deviates from the ground truth, struggling to capture the correct probability mass at specific interatomic distances. In contrast, the iDEM+CVSI model produces a distribution that better aligns with the ground truth, demonstrating that the lower-variance estimator allows the model to learn the correct internal geometry of the system.

5 Conclusion

In this work, we addressed the critical challenge of high estimator variance in score-based models where an energy function is accessible, which dictates sample complexity and can degrade sample quality. By framing score estimation within the principled framework of control variates, we derived the **Control Variate Score Identity (CVSI)**, a unified formulation that encompasses both the Denoising Score Identity and the Target Score Identity as special cases. Moreover, we theoretically established an optimal time-dependent control coefficient $c^*(t)$ that strictly minimizes the variance of the score estimate across all noise levels. Our empirical results demonstrate that our CVSI is a robust, low-variance “plug-in” estimator. Whether applied to data-free training algorithms like iDEM or used to enhance reverse-time diffusion sampling, it scales effectively to high-dimensional systems, while significantly reducing the number of posterior samples required for accurate estimation. We believe that our framework paves the way for more efficient sampling from unnormalized densities and more robust diffusion-based sampling and training in scientific applications.

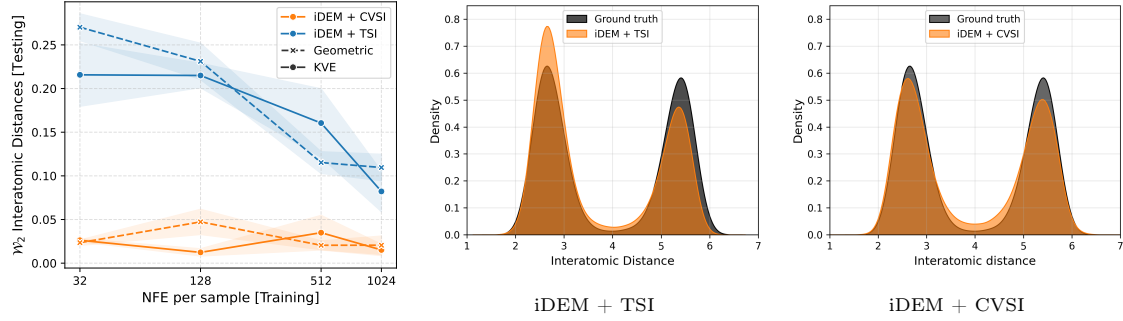


Figure 4: Performance comparison of iDEM with TSI (original) and with our CVS1 on the Double-Well potential with 4 particles (DW-4), using two different schedules, the original geometric schedule (Akhound-Sadegh et al., 2024) and the well-established KVE schedule by (Karras et al., 2022). The left-most plot shows the Wasserstein-2 distance (W_2) between the distributions, generated and ground truth, of the interatomic distances as a function of the number of energy function evaluations (NFE) used per training sample. The two rightmost plots show histograms representing the distributions of the interatomic distances of the generated and reference test data, using the original iDEM with TSI (left) and iDEM with our CVS1 estimator (right) after training with 128 NFE per training sample.

References

Tara Akhoud-Sadegh, Jarrid Rector-Brooks, Avishek Joey Bose, Sarthak Mittal, Pablo Lemos, Cheng-Hao Liu, Marcin Sendera, Siamak Ravanbakhsh, Gauthier Gidel, Yoshua Bengio, Nikolay Malkin, and Alexander Tong. Iterated denoising energy matching for sampling from Boltzmann densities. In *International Conference on Machine Learning*, 2024.

Michael S Albergo, Gurtej Kanwar, and Phiala E Shanahan. Flow-based generative models for markov chain monte carlo in lattice field theory. *Physical Review D*, 100(3):034515, 2019.

Julius Berner, Lorenz Richter, and Karen Ullrich. An optimal control perspective on diffusion-based generative modeling. *Transactions on Machine Learning Research*, 2024. ISSN 2835-8856. URL <https://openreview.net/forum?id=oYIjw37pTP>.

Valentin De Bortoli, Michael Hutchinson, Peter Wirnsberger, and Arnaud Doucet. Target score matching. *arXiv preprint arXiv:2402.08667*, 2024.

Bradley Efron. Tweedie’s formula and selection bias. *Journal of the American Statistical Association*, 106(496):1602–1614, 2011.

Louis Grenioux, Maxence Noble, Marylou Gabré, and Alain Oliviero Durmus. Stochastic localization via iterative posterior sampling. In *International Conference on Machine Learning*, pages 16337–16376. PMLR, 2024.

Aaron J Havens, Benjamin Kurt Miller, Bing Yan, Carles Domingo-Enrich, Anuroop Sriram, Daniel S. Levine, Brandon M Wood, Bin Hu, Brandon Amos, Brian Karrer, Xiang Fu, Guan-Horng Liu, and Ricky T. Q. Chen. Adjoint sampling: Highly scalable diffusion samplers via adjoint matching. In

Forty-second International Conference on Machine Learning, 2025. URL <https://openreview.net/forum?id=6Eg10rHmg2>.

Jonathan Ho, Ajay Jain, and Pieter Abbeel. Denoising diffusion probabilistic models. In H. Larochelle, M. Ranzato, R. Hadsell, M.F. Balcan, and H. Lin, editors, *Advances in Neural Information Processing Systems*, volume 33, pages 6840–6851. Curran Associates, Inc., 2020. URL https://proceedings.neurips.cc/paper_files/paper/2020/file/4c5bcfec8584af0d967f1ab10179ca4b-Paper.pdf.

Xunpeng Huang, Hanze Dong, Yifan HAO, Yian Ma, and Tong Zhang. Reverse diffusion monte carlo. In *The Twelfth International Conference on Learning Representations*, 2024. URL <https://openreview.net/forum?id=kIPEyMSdFV>.

John Jumper, Richard Evans, Alexander Pritzel, Tim Green, Michael Figurnov, Olaf Ronneberger, Kathryn Tunyasuvunakool, Russ Bates, Augustin Žídek, Anna Potapenko, Alex Bridgland, Clemens Meyer, Simon A. A. Kohl, Andrew J. Ballard, Andrew Cowie, Bernardino Romera-Paredes, Stanislav Nikolov, Rishabh Jain, Jonas Adler, Trevor Back, Stig Petersen, David Reiman, Ellen Clancy, Michal Zielinski, Martin Steinegger, Michalina Pacholska, Tamas Berghammer, Sebastian Bodenstein, David Silver, Oriol Vinyals, Andrew W. Senior, Koray Kavukcuoglu, Pushmeet Kohli, and Demis Hassabis. Highly accurate protein structure prediction with alphafold. *Nature*, 596(7873):583–589, August 2021. ISSN 1476-4687. doi: 10.1038/s41586-021-03819-2. URL <https://doi.org/10.1038/s41586-021-03819-2>.

Khaled Kahouli, Winfried Ripken, Stefan Gugler, Oliver T Unke, Klaus-Robert Müller, and Shinichi Nakajima. Disentangling total-variance and signal-to-noise-ratio improves diffusion models. *arXiv preprint arXiv:2502.08598*, 2025.

Tero Karras, Miika Aittala, Timo Aila, and Samuli Laine. Elucidating the design space of diffusion-based generative models. In Alice H. Oh, Alekh Agarwal, Danielle Belgrave, and Kyunghyun Cho, editors, *Advances in Neural Information Processing Systems*, 2022. URL <https://openreview.net/forum?id=k7FuTOWM0c7>.

Joohwan Ko and Tomas Geffner. Latent target score matching, with an application to simulation-based inference. In *Machine Learning and the Physical Sciences Workshop, NeurIPS*, 2025.

Christiane Lemieux. Control variates. *Wiley StatsRef: Statistics Reference Online*, pages 1–8, 2014.

Kim A Nicoli, Shinichi Nakajima, Nils Strothoff, Wojciech Samek, Klaus-Robert Müller, and Pan Kessel. Asymptotically unbiased estimation of physical observables with neural samplers. *Physical Review E*, 101(2):023304, 2020.

Frank Noé, Simon Olsson, Jonas Köhler, and Hao Wu. Boltzmann generators: Sampling equilibrium states of many-body systems with deep learning. *Science*, 365(6457):eaaw1147, 2019. doi: 10.1126/science.aaw1147.

Angus Phillips, Hai-Dang Dau, Michael John Hutchinson, Valentin De Bortoli, George Deligiannidis, and Arnaud Doucet. Particle denoising diffusion sampler. In *Proceedings of the 41st International Conference on Machine Learning*, 2024.

Herbert E Robbins. An empirical bayes approach to statistics. In *Breakthroughs in Statistics: Foundations and basic theory*, pages 388–394. Springer, 1992.

Jascha Sohl-Dickstein, Eric Weiss, Niru Maheswaranathan, and Surya Ganguli. Deep unsupervised learning using nonequilibrium thermodynamics. In Francis Bach and David Blei, editors, *Proceedings of the 32nd International Conference on Machine Learning*, volume 37 of *Proceedings of Machine Learning Research*, pages 2256–2265, Lille, France, 07–09 Jul 2015. PMLR. URL <https://proceedings.mlr.press/v37/sohl-dickstein15.html>.

Yang Song, Jascha Sohl-Dickstein, Diederik P Kingma, Abhishek Kumar, Stefano Ermon, and Ben Poole. Score-based generative modeling through stochastic differential equations. In *International Conference on Learning Representations*, 2021. URL <https://openreview.net/forum?id=PxTIG12RRHS>.

Francisco Vargas, Will Sussman Grathwohl, and Arnaud Doucet. Denoising diffusion samplers. In *The Eleventh International Conference on Learning Representations*, 2023. URL <https://openreview.net/forum?id=8pvnfTAbu1f>.

Pascal Vincent. A connection between score matching and denoising autoencoders. *Neural Computation*, 23(7):1661–1674, 2011. doi: 10.1162/NECO_a_00142.

Qinsheng Zhang and Yongxin Chen. Path integral sampler: A stochastic control approach for sampling. In *International Conference on Learning Representations*, 2022. URL https://openreview.net/forum?id=_uCb2ynRu7Y.

Appendix

A Proof of Eq (5)

In the following, we aim to prove that:

$$\nabla_{\mathbf{x}} \log q_t(\mathbf{x}) = \frac{1}{a(t)} \mathbb{E}_{q(\mathbf{x}(0)|\mathbf{x}(t))} [\nabla_{\mathbf{x}} \log p(\mathbf{x})]. \quad (20)$$

The proof can be performed using either Bayes' rule, see Appendix A.1, or integration by parts, see Appendix A.2.

A.1 Derivation using Bayes' rule:

Starting with the DSI identity:

$$\nabla_{\mathbf{x}} \log q_t(\mathbf{x}) \stackrel{\text{DSI}}{=} \mathbb{E}_{q(\mathbf{x}(0)|\mathbf{x}(t))} [\nabla_{\mathbf{x}(t)} \log q(\mathbf{x}(t)|\mathbf{x}(0))] \quad (21)$$

$$\stackrel{\text{Gauss. sym.}}{=} \mathbb{E}_{q(\mathbf{x}(0)|\mathbf{x}(t))} \left[-\frac{1}{a(t)} \nabla_{\mathbf{x}(0)} \log q(\mathbf{x}(t)|\mathbf{x}(0)) \right] \quad (22)$$

$$\stackrel{\text{Bayes' rule}}{=} -\frac{1}{a(t)} \mathbb{E}_{q(\mathbf{x}(0)|\mathbf{x}(t))} [\nabla_{\mathbf{x}(0)} \log q(\mathbf{x}(0)|\mathbf{x}(t)) + \nabla_{\mathbf{x}(0)} \log q_t(\mathbf{x}(t)) - \nabla_{\mathbf{x}(0)} \log p(\mathbf{x}(0))] \quad (23)$$

$$= -\frac{1}{a(t)} (\mathbb{E}_{q(\mathbf{x}(0)|\mathbf{x}(t))} [\nabla_{\mathbf{x}(0)} \log q(\mathbf{x}(0)|\mathbf{x}(t))] - \mathbb{E}_{q(\mathbf{x}(0)|\mathbf{x}(t))} [\nabla_{\mathbf{x}} \log p(\mathbf{x})]) \quad (24)$$

$$= \frac{1}{a(t)} \mathbb{E}_{q(\mathbf{x}(0)|\mathbf{x}(t))} [\nabla_{\mathbf{x}} \log p(\mathbf{x})], \quad (25)$$

where in step (24) we use:

$$\mathbb{E}_{q(\mathbf{x}(0)|\mathbf{x}(t))} [\nabla_{\mathbf{x}(0)} \log q(\mathbf{x}(0)|\mathbf{x}(t))] = \int q(\mathbf{x}(0)|\mathbf{x}(t)) \frac{\nabla_{\mathbf{x}(0)} q(\mathbf{x}(0)|\mathbf{x}(t))}{q(\mathbf{x}(0)|\mathbf{x}(t))} d\mathbf{x}(0) \quad (26)$$

$$= \int \nabla_{\mathbf{x}(0)} q(\mathbf{x}(0)|\mathbf{x}(t)) d\mathbf{x}(0) \quad (27)$$

$$\stackrel{\text{Gradient theorem}}{=} 0, \quad (28)$$

and in step (22) we use the Gaussian symmetry property:

$$q(\mathbf{x}(t)|\mathbf{x}(0)) = \mathcal{N}(\mathbf{x}(t); a(t)\mathbf{x}(0), b(t)^2 I), \quad (29)$$

$$\nabla_{\mathbf{x}(0)} \log q(\mathbf{x}(t)|\mathbf{x}(0)) = \frac{a(t)(\mathbf{x}(t) - a(t)\mathbf{x}(0))}{b(t)^2}, \quad (30)$$

$$\nabla_{\mathbf{x}(t)} \log q(\mathbf{x}(t)|\mathbf{x}(0)) = -\frac{\mathbf{x}(t) - a(t)\mathbf{x}(0)}{b(t)^2} \quad (31)$$

$$= -\frac{1}{a(t)} \nabla_{\mathbf{x}(0)} \log q(\mathbf{x}(t)|\mathbf{x}(0)). \quad (32)$$

A.2 Derivation using integration by parts

We start with the definition of the marginal $q_t(\mathbf{x}(t))$:

$$\begin{aligned}
\nabla_{\mathbf{x}(t)} \log q_t(\mathbf{x}(t)) &= \frac{1}{q_t(\mathbf{x}(t))} \nabla_{\mathbf{x}(t)} \int q(\mathbf{x}(t)|\mathbf{x}(0)) p(\mathbf{x}(0)) d\mathbf{x}(0) \\
&\stackrel{\text{(Leibniz rule)}}{=} \frac{1}{q_t(\mathbf{x}(t))} \int (\nabla_{\mathbf{x}(t)} q(\mathbf{x}(t)|\mathbf{x}(0))) p(\mathbf{x}(0)) d\mathbf{x}(0) \\
&= \frac{1}{q_t(\mathbf{x}(t))} \int q(\mathbf{x}(t)|\mathbf{x}(0)) (\nabla_{\mathbf{x}(t)} \log q(\mathbf{x}(t)|\mathbf{x}(0))) p(\mathbf{x}(0)) d\mathbf{x}(0) \\
&= \left(\mathbb{E}_{q(\mathbf{x}(0)|\mathbf{x}(t))} [\nabla_{\mathbf{x}(t)} \log q(\mathbf{x}(t)|\mathbf{x}(0))] \quad (\text{DSI identity}) \right) \\
&\stackrel{\text{(Gaussian sym. Eq. (32))}}{=} \frac{1}{q_t(\mathbf{x}(t))} \int q(\mathbf{x}(t)|\mathbf{x}(0)) \left(-\frac{1}{a(t)} \nabla_{\mathbf{x}(0)} \log q(\mathbf{x}(t)|\mathbf{x}(0)) \right) p(\mathbf{x}(0)) d\mathbf{x}(0) \\
&= -\frac{1}{a(t)q_t(\mathbf{x}(t))} \int (\nabla_{\mathbf{x}(0)} q(\mathbf{x}(t)|\mathbf{x}(0))) p(\mathbf{x}(0)) d\mathbf{x}(0) \\
&\stackrel{\text{(Integ. by parts)}}{=} \frac{1}{a(t)q_t(\mathbf{x}(t))} \int q(\mathbf{x}(t)|\mathbf{x}(0)) (\nabla_{\mathbf{x}(0)} p(\mathbf{x}(0))) d\mathbf{x}(0) \\
&= \frac{1}{a(t)q_t(\mathbf{x}(t))} \int q(\mathbf{x}(t)|\mathbf{x}(0)) p(\mathbf{x}(0)) (\nabla_{\mathbf{x}(0)} \log p(\mathbf{x}(0))) d\mathbf{x}(0) \\
&= \frac{1}{a(t)} \int q(\mathbf{x}(0)|\mathbf{x}(t)) \nabla_{\mathbf{x}(0)} \log p(\mathbf{x}(0)) d\mathbf{x}(0) \\
&= \frac{1}{a(t)} \mathbb{E}_{q(\mathbf{x}(0)|\mathbf{x}(t))} [\nabla_{\mathbf{x}(0)} \log p(\mathbf{x}(0))].
\end{aligned}$$

B Derivation of the Interpolated Estimator

We start with the control variate estimator from Eq. (8):

$$\nabla_{\mathbf{x}} \log q_t(\mathbf{x}) = \mathbb{E}_{q(\mathbf{x}(0)|\mathbf{x}(t))} \left[\frac{1}{a(t)} \nabla_{\mathbf{x}} \log p(\mathbf{x}) - c(t) \nabla_{\mathbf{x}(0)} \log q(\mathbf{x}(0)|\mathbf{x}(t)) \right] \quad (33)$$

$$\stackrel{\text{Bayes' rule}}{=} \mathbb{E}_{q(\mathbf{x}(0)|\mathbf{x}(t))} \left[\frac{1}{a(t)} \nabla_{\mathbf{x}} \log p(\mathbf{x}) - c(t) (\nabla_{\mathbf{x}} \log p(\mathbf{x}) + \nabla_{\mathbf{x}(0)} \log q(\mathbf{x}(t)|\mathbf{x}(0))) \right] \quad (34)$$

$$= \mathbb{E}_{q(\mathbf{x}(0)|\mathbf{x}(t))} \left[\left(\frac{1}{a(t)} - c(t) \right) \nabla_{\mathbf{x}} \log p(\mathbf{x}) - c(t) \nabla_{\mathbf{x}(0)} \log q(\mathbf{x}(t)|\mathbf{x}(0)) \right] \quad (35)$$

$$\stackrel{\text{Gauss. sym.}}{=} \mathbb{E}_{q(\mathbf{x}(0)|\mathbf{x}(t))} \left[\left(\frac{1}{a(t)} - c(t) \right) \nabla_{\mathbf{x}} \log p(\mathbf{x}) + c(t) a(t) \nabla_{\mathbf{x}(t)} \log q(\mathbf{x}(t)|\mathbf{x}(0)) \right] \quad (36)$$

$$= \frac{(1 - c(t) a(t))}{a(t)} \mathbb{E}_{q(\mathbf{x}(0)|\mathbf{x}(t))} [\nabla_{\mathbf{x}} \log p(\mathbf{x})] + c(t) a(t) \mathbb{E}_{q(\mathbf{x}(0)|\mathbf{x}(t))} [\nabla_{\mathbf{x}(t)} \log q(\mathbf{x}(t)|\mathbf{x}(0))]. \quad (37)$$

C Derivation of the Optimal Control Coefficient

C.1 Unbiased score estimator

To show that the estimator in Eq. (8) is unbiased, we need to show that

$$\mathbb{E}[g(\mathbf{x}(0)) - c(t)(h(\mathbf{x}(0)) - \mathbb{E}[h(\mathbf{x}(0))])] = \mathbb{E}_{q(\mathbf{x}(0)|\mathbf{x}(t))}[g(\mathbf{x}(0))].$$

Starting with the proposed estimator, we have:

$$\begin{aligned} \mathbb{E}[g(\mathbf{x}(0)) - c(t)(h(\mathbf{x}(0)) - \mathbb{E}[h(\mathbf{x}(0))])] &= \mathbb{E}[g(\mathbf{x}(0))] - \mathbb{E}[c(t)(h(\mathbf{x}(0)) - \mathbb{E}[h(\mathbf{x}(0))])] \\ &= \mathbb{E}[g(\mathbf{x}(0))] - c(t) \cdot (\mathbb{E}[h(\mathbf{x}(0))] - \mathbb{E}[\mathbb{E}[h(\mathbf{x}(0))]]) \\ &= \mathbb{E}[g(\mathbf{x}(0))] - c(t) \cdot (\mathbb{E}[h(\mathbf{x}(0))] - \mathbb{E}[h(\mathbf{x}(0))]) \\ &= \mathbb{E}[g(\mathbf{x}(0))], \end{aligned}$$

which proves that the estimator is unbiased.

C.2 Derivation of $c^*(t)$

Let the control variate estimator for the integrand g be $g_c = g - c(h - \mathbb{E}[h])$. We want to find the value of c that minimizes the variance of g_c . The variance is given by:

$$\begin{aligned} \text{Var}(g_c) &= \text{Var}(g - c(h - \mathbb{E}[h])) \\ &\stackrel{\text{Var}(A-B)}{=} \text{Var}(g) + \text{Var}(c(h - \mathbb{E}[h])) - 2\text{Cov}(g, c(h - \mathbb{E}[h])) \\ &= \text{Var}(g) + c^2\text{Var}(h - \mathbb{E}[h]) - 2c\text{Cov}(g, h - \mathbb{E}[h]) \\ &\stackrel{\mathbb{E}[h] \text{ is const.}}{=} \text{Var}(g) + c^2\text{Var}(h) - 2c\text{Cov}(g, h). \end{aligned}$$

This expression for the variance is a quadratic function of c . To find the minimum, we take the derivative with respect to c and set it to zero:

$$\begin{aligned} \frac{d}{dc}\text{Var}(g_c) &= \frac{d}{dc}(\text{Var}(g) + c^2\text{Var}(h) - 2c\text{Cov}(g, h)) \\ &= 2c\text{Var}(h) - 2\text{Cov}(g, h). \end{aligned}$$

Setting to zero $\implies 2c^*\text{Var}(h) = 2\text{Cov}(g, h)$,

$$c^* = \frac{\text{Cov}(g, h)}{\text{Var}(h)}.$$

Since the second derivative, $2\text{Var}(h)$, is positive, this value of c^* corresponds to a minimum, which completes the proof.

C.3 Computationally Tractable Reformulation for $c^*(t)$

We have:

- $g = a(t)^{-1}\nabla_{\mathbf{x}} \log p(\mathbf{x})$
- $h = \nabla_{\mathbf{x}(0)} \log q(\mathbf{x}(0)|\mathbf{x}(t))$

- $k = \nabla_{\mathbf{x}(0)} \log q(\mathbf{x}(t) | \mathbf{x}(0))$

To make the derivation easy we consider the rescaled version $\tilde{g}(t) = a(t)g(t) = \nabla_{\mathbf{x}} \log p(\mathbf{x})$, and therefore we get:

$$c^* = \frac{1}{a(t)} \frac{\text{Cov}(\tilde{g}, h)}{\text{Var}(h)}.$$

From the proof of Proposition 1, we know these terms are related by Bayes' rule such that $h = \tilde{g} + k$. All expectations, variances, and covariances are taken with respect to the posterior, $q(\mathbf{x}(0) | \mathbf{x}(t))$. Therefore, we can re-write $c^*(t)$ as:

Numerator:

$$\begin{aligned} \text{Cov}(\tilde{g}, h) &= \text{Cov}(\tilde{g}, \tilde{g} + k) \\ &= \text{Cov}(\tilde{g}, \tilde{g}) + \text{Cov}(\tilde{g}, k) \\ &= \text{Var}(\tilde{g}) + \text{Cov}(\tilde{g}, k). \end{aligned}$$

Denominator:

$$\begin{aligned} \text{Var}(h) &= \text{Var}(\tilde{g} + k) \\ &= \text{Var}(\tilde{g}) + \text{Var}(k) + 2\text{Cov}(\tilde{g}, k). \end{aligned}$$

Therefore, we obtain the reformulated control coefficient:

$$c^*(t) = \frac{1}{a(t)} \frac{\text{Var}(\nabla_{\mathbf{x}} \log p(\mathbf{x})) + \text{Cov}(\nabla_{\mathbf{x}} \log p(\mathbf{x}), \nabla_{\mathbf{x}(0)} \log q_{t|0})}{\text{Var}(\nabla_{\mathbf{x}} \log p(\mathbf{x})) + \text{Var}(\nabla_{\mathbf{x}(0)} \log q_{t|0}) + 2\text{Cov}(\nabla_{\mathbf{x}} \log p(\mathbf{x}), \nabla_{\mathbf{x}(0)} \log q_{t|0})}, \quad (38)$$

where $q_{t|0} = q(x(t) | x(0))$. Moreover, by using the identity:

$$\nabla_{\mathbf{x}(0)} \log q_{t|0} = -a(t) \nabla_{\mathbf{x}(t)} \log q_{t|0}, \quad (39)$$

we get the final result:

$$\begin{aligned} c^*(t) &= \frac{1}{a(t)} \frac{\text{Var}(\nabla_{\mathbf{x}} \log p(\mathbf{x})) - a(t)\text{Cov}(\nabla_{\mathbf{x}} \log p(\mathbf{x}), \nabla_{\mathbf{x}(t)} \log q_{t|0})}{\text{Var}(\nabla_{\mathbf{x}} \log p(\mathbf{x})) + a(t)^2 \text{Var}(\nabla_{\mathbf{x}(t)} \log q_{t|0}) - 2a(t)\text{Cov}(\nabla_{\mathbf{x}} \log p(\mathbf{x}), \nabla_{\mathbf{x}(t)} \log q_{t|0})} \\ &= \frac{\text{Var}(\nabla_{\mathbf{x}} \log p(\mathbf{x})) - a(t)\text{Cov}(\nabla_{\mathbf{x}} \log p(\mathbf{x}), \nabla_{\mathbf{x}(t)} \log q_{t|0})}{a(t) \text{Var}(\nabla_{\mathbf{x}} \log p(\mathbf{x})) + a(t)^3 \text{Var}(\nabla_{\mathbf{x}(t)} \log q_{t|0}) - 2a(t)^2 \text{Cov}(\nabla_{\mathbf{x}} \log p(\mathbf{x}), \nabla_{\mathbf{x}(t)} \log q_{t|0})}. \end{aligned} \quad (40)$$

D Derivation and Reframing of Previous Methods

D.1 iDEM

Let the scaled variable be $\tilde{\mathbf{x}}(t) = \mathbf{x}(t)/a(t)$, and the SNR ratio be $\gamma(t) = a(t)/b(t)$. Using the proposal distribution $\pi_{\text{iDEM}}(\mathbf{x}(0) | \tilde{\mathbf{x}}(t)) = \mathcal{N}(\mathbf{x}(0); \tilde{\mathbf{x}}(t), \gamma(t)^{-2})$, the iDEM estimator (Akhound-Sadegh et al., 2024) is defined as:

$$\nabla_{\tilde{\mathbf{x}}(t)} \log \tilde{q}_t(\tilde{\mathbf{x}}(t)) = \nabla_{\tilde{\mathbf{x}}(t)} \log \mathbb{E}_{\pi_{\text{iDEM}}(\mathbf{x}(0) | \tilde{\mathbf{x}}(t))} [p(\mathbf{x}(0))] \quad (41)$$

$$= \frac{\mathbb{E}_{\pi_{\text{iDEM}}(\mathbf{x}(0) | \tilde{\mathbf{x}}(t))} [\nabla_{\mathbf{x}(0)} p(\mathbf{x}(0))]}{\mathbb{E}_{\pi_{\text{iDEM}}(\mathbf{x}(0) | \tilde{\mathbf{x}}(t))} [p(\mathbf{x}(0))]}, \quad (42)$$

which can be developed as follows:

$$\begin{aligned} & \frac{\mathbb{E}_{\pi_{\text{iDEM}}(\mathbf{x}(0)|\tilde{\mathbf{x}}(t))} [\nabla_{\mathbf{x}(0)} p(\mathbf{x}(0))] }{\mathbb{E}_{\pi_{\text{iDEM}}(\mathbf{x}(0)|\tilde{\mathbf{x}}(t))} [p(\mathbf{x}(0))] } \\ &= \frac{1}{\tilde{q}_t(\tilde{\mathbf{x}}(t))} \int \nabla_{\mathbf{x}(0)} p(\mathbf{x}(0)) \pi_{\text{iDEM}}(\mathbf{x}(0)|\tilde{\mathbf{x}}(t)) d\mathbf{x}(0) \end{aligned} \quad (43)$$

$$= \int \frac{p(\mathbf{x}(0))}{\tilde{q}_t(\tilde{\mathbf{x}}(t))} \nabla_{\mathbf{x}(0)} \log p(\mathbf{x}(0)) \pi_{\text{iDEM}}(\mathbf{x}(0)|\tilde{\mathbf{x}}(t)) d\mathbf{x}(0) \quad (44)$$

$$= \mathbb{E}_{\pi_{\text{iDEM}}(\mathbf{x}(0)|\tilde{\mathbf{x}}(t))} \left[\frac{p(\mathbf{x}(0))}{\tilde{q}_t(\tilde{\mathbf{x}}(t))} \nabla_{\mathbf{x}(0)} \log p(\mathbf{x}(0)) \right] \quad (45)$$

$$= \mathbb{E}_{\pi_{\text{iDEM}}(\mathbf{x}(0)|\tilde{\mathbf{x}}(t))} \left[\frac{p(\mathbf{x}(0)) \pi_{\text{iDEM}}(\mathbf{x}(0)|\tilde{\mathbf{x}}(t))}{\tilde{q}_t(\tilde{\mathbf{x}}(t)) \pi_{\text{iDEM}}(\mathbf{x}(0)|\tilde{\mathbf{x}}(t))} \nabla_{\mathbf{x}(0)} \log p(\mathbf{x}(0)) \right] \quad (46)$$

$$= \mathbb{E}_{\pi_{\text{iDEM}}(\mathbf{x}(0)|\tilde{\mathbf{x}}(t))} \left[\frac{p(\mathbf{x}(0)) \tilde{q}(\tilde{\mathbf{x}}(t)|\mathbf{x}(0))}{\tilde{q}_t(\tilde{\mathbf{x}}(t)) \pi_{\text{iDEM}}(\mathbf{x}(0)|\tilde{\mathbf{x}}(t))} \nabla_{\mathbf{x}(0)} \log p(\mathbf{x}(0)) \right] \quad (47)$$

$$= \mathbb{E}_{\pi_{\text{iDEM}}(\mathbf{x}(0)|\tilde{\mathbf{x}}(t))} \left[\frac{\tilde{q}(\mathbf{x}(0)|\tilde{\mathbf{x}}(t))}{\pi_{\text{iDEM}}(\mathbf{x}(0)|\tilde{\mathbf{x}}(t))} \nabla_{\mathbf{x}(0)} \log p(\mathbf{x}(0)) \right] \quad (48)$$

$$\tilde{q}(\mathbf{x}(0)|\tilde{\mathbf{x}}(t)) \stackrel{q(\mathbf{x}(0)|\mathbf{x}(t))}{=} \mathbb{E}_{\pi_{\text{iDEM}}(\mathbf{x}(0)|\tilde{\mathbf{x}}(t))} \left[\frac{q(\mathbf{x}(0)|\mathbf{x}(t))}{\pi_{\text{iDEM}}(\mathbf{x}(0)|\tilde{\mathbf{x}}(t))} \nabla_{\mathbf{x}(0)} \log p(\mathbf{x}(0)) \right] \quad (49)$$

$$= \mathbb{E}_{q(\mathbf{x}(0)|\mathbf{x}(t))} [\nabla_{\mathbf{x}(0)} \log p(\mathbf{x}(0))], \quad (50)$$

where we use the following equalities:

$$\pi_{\text{iDEM}}(\mathbf{x}(0)|\tilde{\mathbf{x}}(t)) = \mathcal{N}(\mathbf{x}(0); \tilde{\mathbf{x}}(t), \gamma(t)^{-2}) = \tilde{q}(\tilde{\mathbf{x}}(t)|\mathbf{x}(0)), \quad (51)$$

and

$$\tilde{q}(\mathbf{x}(0)|\tilde{\mathbf{x}}(t)) = \frac{\tilde{q}(\tilde{\mathbf{x}}(t)|\mathbf{x}(0)) p(\mathbf{x}(0))}{\tilde{q}_t(\tilde{\mathbf{x}}(t))} \quad (52)$$

$$\stackrel{\text{(Change of var.)}}{=} \frac{a(t)^D q(\mathbf{x}(t)|\mathbf{x}(0)) p(\mathbf{x}(0))}{a(t)^D q_t(\mathbf{x}(t))} \quad (53)$$

$$= \frac{q(\mathbf{x}(t)|\mathbf{x}(0)) p(\mathbf{x}(0))}{q_t(\mathbf{x}(t))} \quad (54)$$

$$= q(\mathbf{x}(0)|\mathbf{x}(t)), \quad (55)$$

where D is the dimensionality of the data. While the above derivation holds for any schedule, the iDEM estimator is primarily associated with the Variance Exploding (VE) framework. However, we

can relate the estimator for the scaled variable $\tilde{\mathbf{x}}(t)$ to the unscaled original variable $\mathbf{x}(t)$ as follows:

$$\nabla_{\mathbf{x}(t)} \log q_t(\mathbf{x}(t)) = \nabla_{\mathbf{x}(t)} \log \left(\frac{1}{a(t)^D} \tilde{q}_t(\tilde{\mathbf{x}}(t)) \right) \quad (56)$$

$$= \nabla_{\mathbf{x}(t)} \log \tilde{q}_t(\tilde{\mathbf{x}}(t)) \quad (57)$$

$$= \frac{1}{a(t)} \nabla_{\tilde{\mathbf{x}}(t)} \log \tilde{q}_t(\tilde{\mathbf{x}}(t)) \quad (58)$$

$$= \frac{1}{a(t)} \mathbb{E}_{\pi_{\text{iDEM}}(\mathbf{x}(0)|\tilde{\mathbf{x}}(t))} \left[\frac{q(\mathbf{x}(0)|\mathbf{x}(t))}{\pi_{\text{iDEM}}(\mathbf{x}(0)|\tilde{\mathbf{x}}(t))} \nabla_{\mathbf{x}(0)} \log p_0(\mathbf{x}(0)) \right] \quad (59)$$

$$= \frac{1}{a(t)} \mathbb{E}_{q(\mathbf{x}(0)|\mathbf{x}(t))} [\nabla_{\mathbf{x}(0)} \log p_0(\mathbf{x}(0))]. \quad (60)$$

Eq. 49 and its unscaled version Eq. 59 show that the estimator used in iDEM is an importance sampling (IS) estimator for the target score identity from Eq. (5), with importance weights:

$$w_{\text{iDEM}}(\mathbf{x}(t), t) = \frac{p(\mathbf{x}(0))}{\tilde{q}_t(\tilde{\mathbf{x}}(t))} \quad (61)$$

$$= \frac{q(\mathbf{x}(0)|\mathbf{x}(t))}{\pi_{\text{iDEM}}(\mathbf{x}(0)|\tilde{\mathbf{x}}(t))} \quad (62)$$

$$= \frac{q(\mathbf{x}(0)|\mathbf{x}(t))}{\tilde{q}(\tilde{\mathbf{x}}(t)|\mathbf{x}(0))} \quad (63)$$

$$\stackrel{\text{(Change of var.)}}{=} \frac{q(\mathbf{x}(0)|\mathbf{x}(t))}{a(t)^D q(\mathbf{x}(t)|\mathbf{x}(0))} \quad (64)$$

$$= \frac{p(\mathbf{x}(0))}{a(t)^D q_t(\mathbf{x}(t))}. \quad (65)$$

The variance of this importance weight is lowest when the proposal distribution $\pi_{\text{iDEM}}(\mathbf{x}(0)|\tilde{\mathbf{x}}(t))$ is a good match for the target posterior $q(\mathbf{x}(0)|\mathbf{x}(t))$, which occurs as $t \rightarrow 0$, where the distributions collapse into sharp Gaussians centered around $\mathbf{x}(t)$. Conversely, the variance is very high when t is large.

E Analytical Solution for Diffused Multivariate Gaussian Mixture Models

We consider a more general case of De Bortoli et al. (2024), where the initial data distribution is modeled as a multivariate Gaussian Mixture Model (GMM) in \mathbb{R}^d :

$$p(\mathbf{x}(0)) = \sum_{i=1}^N \pi^i \mathcal{N}(\mathbf{x}(0); \boldsymbol{\mu}^i, \boldsymbol{\Sigma}^i). \quad (66)$$

We use a superscript i (e.g., $\boldsymbol{\mu}^i$) to denote the i -th component of the mixture model, in order to reserve subscripts for vector or matrix element indexing.

E.1 Derivation of the Marginal Distribution $q(\mathbf{x}(t))$

To find the marginal distribution $q(\mathbf{x}(t))$, we integrate over all possible initial states $\mathbf{x}(0)$:

$$\begin{aligned} q(\mathbf{x}(t)) &= \int q(\mathbf{x}(t)|\mathbf{x}(0))p(\mathbf{x}(0))d\mathbf{x}(0) \\ &= \int \mathcal{N}(\mathbf{x}(t); a(t)\mathbf{x}(0), b(t)^2\mathbf{I}) \left(\sum_{i=1}^N \pi^i \mathcal{N}(\mathbf{x}(0); \boldsymbol{\mu}^i, \boldsymbol{\Sigma}^i) \right) d\mathbf{x}(0) \\ &= \sum_{i=1}^N \pi^i \int \mathcal{N}(\mathbf{x}(t); a(t)\mathbf{x}(0), b(t)^2\mathbf{I}) \mathcal{N}(\mathbf{x}(0); \boldsymbol{\mu}^i, \boldsymbol{\Sigma}^i) d\mathbf{x}(0). \end{aligned}$$

The integral represents the convolution of two multivariate Gaussians, which results in another multivariate Gaussian. The new mean vector and covariance for each component i are:

$$\begin{aligned} \mathbb{E}[\mathbf{x}(t)] &= a(t)\mathbb{E}[\mathbf{x}(0)] + \mathbb{E}[\mathbf{w}] = a(t)\boldsymbol{\mu}^i, \\ \text{Cov}(\mathbf{x}(t)) &= a(t)^2\text{Cov}(\mathbf{x}(0)) + \text{Cov}(\mathbf{w}) = a(t)^2\boldsymbol{\Sigma}^i + b(t)^2\mathbf{I}, \end{aligned}$$

where $\mathbf{w} \sim \mathcal{N}(\mathbf{0}, b(t)^2\mathbf{I})$, and assuming independence between $\mathbf{x}(0)$ and \mathbf{w} . Therefore, we get:

$$q_t(\mathbf{x}) = \sum_{i=1}^N \pi^i \mathcal{N}(\mathbf{x}; \boldsymbol{\mu}^i(t), \boldsymbol{\Sigma}^i(t)), \quad (67)$$

$$\text{where } \boldsymbol{\mu}^i(t) = a(t)\boldsymbol{\mu}^i, \quad (68)$$

$$\text{and } \boldsymbol{\Sigma}^i(t) = a(t)^2\boldsymbol{\Sigma}^i + b(t)^2\mathbf{I}. \quad (69)$$

E.2 Derivation of the Posterior Distribution $q(\mathbf{x}(0)|\mathbf{x}(t))$

We use Bayes' theorem:

$$q(\mathbf{x}(0)|\mathbf{x}(t)) = \frac{q(\mathbf{x}(t)|\mathbf{x}(0))p(\mathbf{x}(0))}{q(\mathbf{x}(t))}.$$

The posterior is proportional to the product of the likelihood and the prior, which is the product of two Gaussians for a single component i :

$$\mathcal{N}(\mathbf{x}(t); a(t)\mathbf{x}(0), b(t)^2\mathbf{I}) \times \mathcal{N}(\mathbf{x}(0); \boldsymbol{\mu}^i, \boldsymbol{\Sigma}^i).$$

Therefore, by applying the standard update rules from the Kalman filtering framework for linear-Gaussian systems, we get the posterior covariance for each component i :

$$\boldsymbol{\Gamma}^i(t) = \left((\boldsymbol{\Sigma}^i)^{-1} + \frac{a(t)^2}{b(t)^2} \mathbf{I} \right)^{-1}, \quad (70)$$

and mean:

$$\boldsymbol{\nu}^i(t) = \boldsymbol{\Gamma}^i(t) \left(\frac{a(t)}{b(t)^2} \mathbf{x}(t) + (\boldsymbol{\Sigma}^i)^{-1} \boldsymbol{\mu}^i \right). \quad (71)$$

Given the above posterior means and covariances, we get the posterior GMM:

$$q(\mathbf{x}(0)|\mathbf{x}(t)) = \sum_{i=1}^N \pi^i(t) \mathcal{N}(\mathbf{x}(0); \boldsymbol{\nu}^i(t), \boldsymbol{\Gamma}^i(t)), \quad (72)$$

with the time-dependent mixture weights $\pi^i(t)$ representing the posterior probabilities of belonging to component i at time t :

$$\pi^i(t) = \frac{\pi^i \mathcal{N}(\mathbf{x}(t); \boldsymbol{\mu}^i(t), \boldsymbol{\Sigma}^i(t))}{\sum_{j=1}^N \pi^j \mathcal{N}(\mathbf{x}(t); \boldsymbol{\mu}^j(t), \boldsymbol{\Sigma}^j(t))}. \quad (73)$$